doi:10.1038/nature10755

Cancer exome analysis reveals a T-cell-dependent mechanism of cancer immunoediting

Hirokazu Matsushita[1]†*, Matthew D. Vesely[1]*, Daniel C. Koboldt[2], Charles G. Rickert[1], Ravindra Uppaluri[3], Vincent J. Magrini[2,4], Cora D. Arthur[1], J. Michael White[1], Yee-Shiuan Chen[1], Lauren K. Shea[1], Jasreet Hundal[2], Michael C. Wendl[2,4], Ryan Demeter[2], Todd Wylie[2], James P. Allison[5,6], Mark J. Smyth[7,8], Lloyd J. Old[9], Elaine R. Mardis[2,4] & Robert D. Schreiber[1]

Cancer immunoediting, the process by which the immune system controls tumour outgrowth and shapes tumour immunogenicity, is comprised of three phases: elimination, equilibrium and escape[1–5]. Although many immune components that participate in this process are known, its underlying mechanisms remain poorly defined. A central tenet of cancer immunoediting is that T-cell recognition of tumour antigens drives the immunological destruction or sculpting of a developing cancer. However, our current understanding of tumour antigens comes largely from analyses of cancers that develop in immunocompetent hosts and thus may have already been edited. Little is known about the antigens expressed in nascent tumour cells, whether they are sufficient to induce protective antitumour immune responses or whether their expression is modulated by the immune system. Here, using massively parallel sequencing, we characterize expressed mutations in highly immunogenic methylcholanthrene-induced sarcomas derived from immunodeficient *Rag2*$^{-/-}$ mice that phenotypically resemble nascent primary tumour cells[1,3,5]. Using class I prediction algorithms, we identify mutant spectrin-β2 as a potential rejection antigen of the d42m1 sarcoma and validate this prediction by conventional antigen expression cloning and detection. We also demonstrate that cancer immunoediting of d42m1 occurs via a T-cell-dependent immunoselection process that promotes outgrowth of pre-existing tumour cell clones lacking highly antigenic mutant spectrin-β2 and other potential strong antigens. These results demonstrate that the strong immunogenicity of an unedited tumour can be ascribed to expression of highly antigenic mutant proteins and show that outgrowth of tumour cells that lack these strong antigens via a T-cell-dependent immunoselection process represents one mechanism of cancer immunoediting.

For this study, we chose two representative, highly immunogenic, unedited methylcholanthrene (MCA)-induced sarcoma cell lines, d42m1 and H31m1, derived from immunodeficient *Rag2*$^{-/-}$ mice[1]. Both grow progressively when transplanted orthotopically into *Rag2*$^{-/-}$ mice, but are rejected when transplanted into naive wild-type mice (Supplementary Figs 1 and 2). Using a modified form of exome sequencing involving complementary DNA (cDNA) capture by mouse exome probes and Illumina deep sequencing (that is, cDNA capture sequencing or cDNA CapSeq), we identified 3,737 somatic, non-synonymous mutations in d42m1 cells (3,398 missense, 221 nonsense, 2 nonstop and 116 splice site mutations) and 2,677 non-synonymous mutations in H31m1 cells (2,391 missense, 160 nonsense, 3 nonstop and 123 splice site mutations) (Fig. 1a and Supplementary Fig. 3 and Supplementary Table 1). The mutations in each cell line were largely distinct—d42m1 and H31m1 share only 119 identical missense mutations (Fig. 1b and Supplementary Table 2)—a result that potentially explains the unique antigenicity of each cell line (Supplementary Fig. 4). Although d42m1 and H31m1 display mutations in known cancer genes[6], the functional effects of these novel mutations remain undefined. Nevertheless, both tumours have cancer-causing mutations in *Kras* (codon 12) and *Trp53* that are frequently observed in human and mouse cancers[7–9] (Supplementary Table 3). The mutation calls were confirmed by independent Roche/454 pyrosequencing of 22 genes using tumour genomic DNA and by documenting their absence in normal cells from the same mouse that developed the tumour (Supplementary Table 4).

Comparing cDNA CapSeq data of d42m1 and H31m1 cells to human cancer genomes[10–17] revealed two similarities. First, 46–47% of mutations in d42m1 and H31m1 are C/A or G/T transversions, which represent chemical-carcinogen signatures[7,13,14] similar to those of lung cancers from smokers (44–46%) but not seen in human cancers induced by other mechanisms (8–16%) (Fig. 1c). Second, the mutation rates of d42m1 and H31m1 are about tenfold higher than those of lung cancers from smokers, but within threefold of hypermutator smoker lung cancers with mutations in DNA repair pathway genes (Fig. 1d). Interestingly, d42m1 and H31m1 also show mutations in DNA repair genes (Supplementary Table 3), although these novel mutations have not been functionally characterized. Thus, mouse MCA-induced sarcomas have qualitative and quantitative genomic similarities to carcinogen-induced human cancers.

When parental d42m1 sarcoma cells were transplanted into naive wild-type mice, approximately 20% of recipients developed escape tumours (Supplementary Fig. 5a, c). Cell lines made from three escape tumours (d42m1-es1, d42m1-es2 and d42m1-es3) formed progressively growing sarcomas when transplanted into naive wild-type recipients (Fig. 2a). In contrast, parental d42m1 tumour cells passaged through *Rag2*$^{-/-}$ mice maintained high immunogenicity (Supplementary Fig. 5b, d). Additional analyses revealed that whereas eight of ten clones of d42m1 were rejected in wild-type mice, two clones (d42m1-T3 and d42m1-T10) grew with kinetics similar to d42m1 escape tumours (Fig. 2a and Supplementary Fig. 6). Thus, the d42m1 cell line consists mostly, but not entirely, of highly immunogenic clones and undergoes immunoediting in wild-type mice. cDNA CapSeq of parental d42m1 cells, clones and escape tumours revealed that all expressed similar numbers of mutations (Supplementary Fig. 7a and Supplementary Table 1) and phylogenetic analysis revealed that all d42m1-derived cells were genomically related to one another but distinct from H31m1 and normal fibroblasts (Supplementary

[1]Department of Pathology and Immunology, Washington University School of Medicine, 660 South Euclid Avenue, St Louis, Missouri 63110, USA. [2]The Genome Institute, Washington University School of Medicine, 660 South Euclid Avenue, St Louis, Missouri 63110, USA. [3]Department of Otolaryngology, Washington University School of Medicine, 660 South Euclid Avenue, St Louis, Missouri 63110, USA. [4]Department of Genetics, Washington University School of Medicine, 660 South Euclid Avenue, St Louis, Missouri 63110, USA. [5]Ludwig Center for Cancer Immunotherapy, Department of Immunology, Memorial Sloan-Kettering Cancer Center, New York, New York 10021, USA. [6]Howard Hughes Medical Institute, Memorial Sloan-Kettering Cancer Center, New York, New York 10021, USA. [7]Cancer Immunology Program, Peter MacCallum Cancer Centre, East Melbourne, 3002 Victoria, Australia. [8]Department of Pathology, University of Melbourne, Parkville, 2010 Victoria, Australia. [9]New York Branch of The Ludwig Institute for Cancer Research at Memorial Sloan-Kettering Cancer Center, New York, New York 10021, USA. †Present address: Department of Immunotherapeutics (Medinet), The University of Tokyo Hospital, 7-3-1 Hongo, Bunkyo-ku, Tokyo 113-8655, Japan.
*These authors contributed equally to this work.

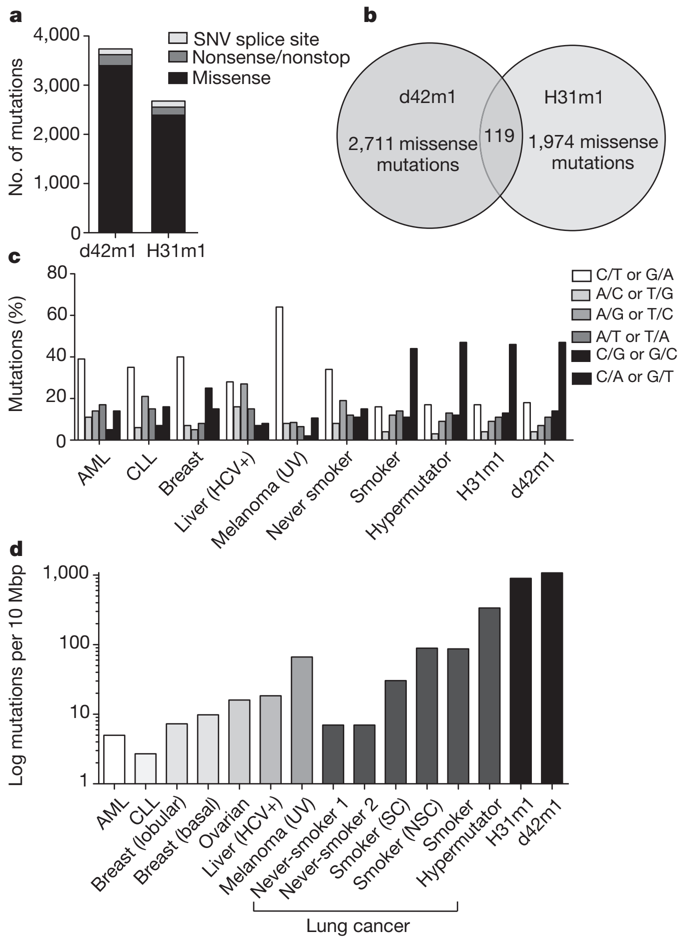

Figure 1 | Unedited MCA-induced sarcomas d42m1 and H31m1 genomically resemble carcinogen-induced human cancers. **a**, Number of non-synonymous mutations in d42m1 and H31m1 tumour cells as detected by cDNA CapSeq. SNV, single nucleotide variant. **b**, Missense mutations compared between d42m1 and H31m1 that had at least 20× sequencing coverage. **c**, Spectrum of DNA nucleotide substitutions detected in d42m1 and H31m1 as compared to previously generated data from human cancers including acute myelogenous leukaemia[10] (AML), chronic lymphocytic leukaemia[16] (CLL), breast cancer (breast lobular[12], breast basal[11]), ovarian cancer (E. R. Mardis *et al.*, manuscript in preparation), liver cancer (hepatitis C virus (HCV)-positive)[15], melanoma (ultraviolet (UV)-induced)[17] and lung cancers (non-small cell (NSC)[13], small cell (SC)[14], never-smoker, smoker and hypermutator (E. R. Mardis *et al.*, manuscript in preparation). **d**, Mutation rates for d42m1, H31m1 and human cancers described in **c** including tumours from never-smoker 1 (bronchioloalveolar carcinoma) and never-smoker 2 (lung adenocarcinoma).

Fig. 7b). However, regressor clones clustered more closely to parental d42m1 cells whereas progressor clones clustered more closely to cells from escape tumours. Thus, the d42m1 tumour cell line consists of a related, but heterogeneous population of tumour cells.

Tumour-specific mutant proteins presented on mouse or human MHC class I molecules are known to represent one class of tumour-specific antigens for $CD8^+$ T cells[18,19]. Therefore, we used *in silico* analysis[20] to assess the theoretical capacities of missense mutations from d42m1-related tumour cells to bind MHC class I proteins. Each d42m1-related cell type expressed many potential high-affinity (half-maximum inhibitory concentration (IC_{50}) < 50 nM; affinity value ($1/IC_{50} \times 100$) >2) epitopes that could bind to H-2D^b or H-2K^b (Fig. 2b). Of these, 39–42 were expressed only in the regressor subset of d42m1-related cells (7–9 for H-2D^b, 30–35 for H-2K^b), including 31 expressed in all regressor cells (Supplementary Table 5). Thus, ~1% of the missense mutations in d42m1 are selectively expressed in rejectable d42m1 clones.

Whereas parental and regressor d42m1 cells stimulated interferon-γ (IFN-γ) release *in vitro* when incubated with a specific $CD8^+$ cytotoxic T lymphocyte (CTL) clone (C3) derived from a wild-type mouse that had rejected parental d42m1 tumour cells (Fig. 3a, b), progressor d42m1 clones, cells from escape tumours or unrelated MCA sarcomas did not. This result demonstrated that all regressor d42m1 tumour cells share a mutation that forms the epitope recognized by C3 CTLs. As recognition of d42m1 regressor cells by C3 CTLs is restricted by H-2D^b (Fig. 3c), we postulated that an R913L mutation in spectrin-β2 produced the most likely target for C3 CTLs because its expression was restricted to d42m1 regressor clones and it formed an epitope that showed high-affinity binding potential to H-2D^b in contrast to the wild-type sequence predicted to bind with low affinity (Fig. 3d and Supplementary Table 5).

To verify the importance of mutant spectrin-β2 on d42m1 antigenicity, we independently identified the tumour antigen recognized by the C3 CTL clone using a T-cell-based expression cloning approach[21]. After three screening rounds, a single positive cDNA was identified encoding a sequence identical to the R913L spectrin-β2 mutant (Fig. 3e). Thus, conventional antigen expression cloning identified the same mutation predicted by the genomic sequencing.

Mutation-specific real-time quantitative polymerase chain reaction with reverse transcription (qRT–PCR) revealed the presence of mutant spectrin-β2 messenger RNA in parental d42m1 tumour cells and regressor d42m1 clones, but not in progressor d42m1 clones or escape tumours (Fig. 3f), nor in normal tissue of the mouse from which the d42m1 tumour was derived (Supplementary Table 4 and Supplementary Fig. 8). Additionally, C3 CTLs discriminated between mutant and wild-type spectrin-β2 peptide sequences when presented on an unrelated H-2D^b-expressing cell line (Fig. 3g). Whereas the mutant (VAVVNQIA<u>L</u>; underline letter indicates the site of mutation) peptide stimulated C3 CTLs in a dose-dependent manner, the wild-type (VAVVNQIA<u>R</u>) peptide did not, even when added in 1,000-fold excess. Using labelled H-2D^b tetramers generated with mutant peptide, mutant spectrin-β2-specific $CD8^+$ T cells accumulated over time in parental d42m1 tumours developing *in vivo* and draining lymph nodes before tumour rejection (Fig. 4a, b). In contrast, no mutant spectrin-β2-specific $CD8^+$ T cells were detected in progressively growing escape tumours or draining lymph nodes. These data demonstrate that mutant spectrin-β2 expressed selectively in a high proportion of unedited d42m1 tumour cells evokes a T-cell response in naive wild-type mice that promotes the elimination of antigen-expressing tumour cells.

To test whether expression of mutant spectrin-β2 was sufficient to drive rejection of d42m1 tumour cells, we enforced expression of either mutant or wild-type spectrin-β2 in d42m1-es3 cells that lack this mutation (Supplementary Fig. 9a) and followed their growth in wild-type mice. Whereas d42m1-es3 tumour cell clones transduced with either control retrovirus or retrovirus encoding wild-type spectrin-β2 (WT.1 and WT.3) grew progressively with growth kinetics similar to unmanipulated d42m1-es3 cells, d42m1-es3 clones expressing mutant spectrin-β2 (mu.6 and mu.14) were rejected in wild-type mice, but not in $Rag2^{-/-}$ mice (Fig. 4c and Supplementary Fig. 9b, c, d). $CD8^+$ T cells specific for mutant spectrin-β2 did not infiltrate d42m1-es3 tumours expressing wild-type spectrin-β2 (WT.3), but were present in d42m1-es3 tumours expressing mutant spectrin-β2 (mu.14) that were rejected in wild-type mice (Fig. 4d). Thus, mutant spectrin-β2 is indeed a major rejection antigen of d42m1 sarcoma cells and d42m1 escape from immune control is the consequence of outgrowth of d42m1 clones that lack expression of dominant rejection antigens.

The possibility that the lack of dominant rejection antigen(s) in a small subset of d42m1 cells was due to epigenetic silencing was ruled out because no spectrin-β2 mutation was (1) found by sequencing genomic DNA from progressor d42m1 clones or escape tumours (Supplementary Table 4) or (2) expressed in d42m1 progressor clones or escape tumours after treatment with inhibitors of methyltransferases and histone deacetylases (Supplementary Fig. 10). We therefore

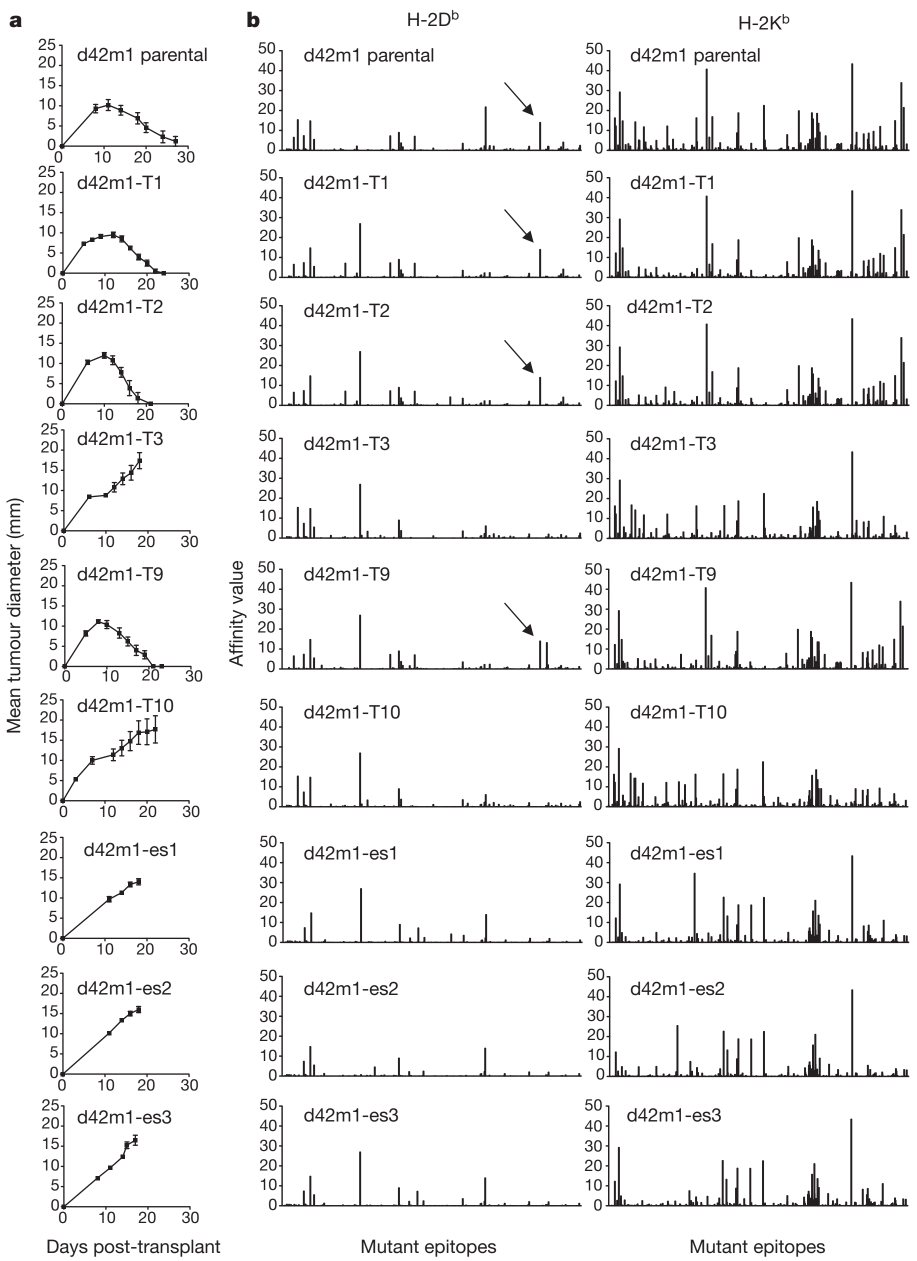

Figure 2 | Affinity value profiles of predicted MHC class I epitopes from tumour-specific mutations. **a**, Growth of d42m1 parental cells, a representative sample of tumour clones, and three escape tumours following transplantation into wild-type mice ($n = 5$, squares). Data are presented as average tumour diameter ± s.e.m. and are representative of three independent experiments. **b**, Missense mutations for each d42m1-related tumour examined in **a** were analysed for potential MHC class I neoepitopes that bind either H-2D^b or H-2K^b. Predicted epitope binding affinities were ultimately expressed as affinity values (1/IC_{50} × 100). Arrows indicate H-2D^b epitopes created by the R913L spectrin-β2 mutant.

asked whether T-cell-dependent immunoselection explained the outgrowth of escape tumours. Specifically, we examined the *in vivo* growth behaviour of a tumour cell mixture containing a vast majority of highly immunogenic, mutant spectrin-β2$^+$ d42m1-T2 cells and a minority of mutant spectrin-β2$^-$ d42m1-T3 progressor cells. To distinguish between the two cell types, we labelled d42m1-T2 with red fluorescent protein (RFP) (modified to eliminate class I epitopes) and d42m1-T3 with green fluorescent protein (GFP) and documented that the labelling did not alter their *in vivo* growth characteristics. We found that we could recapitulate the tumour growth phenotype of parental d42ml at a ratio of 95% d42m1-T2 cells to 5% d42m1-T3 cells (Fig. 4e). At this ratio, 100% of *Rag2*$^{-/-}$ mice and wild-type mice depleted of either CD4$^+$ or CD8$^+$ T cells developed progressively growing tumours (Fig. 4f). In contrast, 5/20 (25%) wild-type mice injected with the tumour cell mixture developed escape tumours, a result that recapitulated the behaviour of parental d42m1. Tumours harvested from *Rag2*$^{-/-}$ mice were comprised of 84% d42m1-T2 cells and 14% d42m1-T3 cells (Fig. 4h) and expressed mutant spectrin-β2 (Fig. 4g), that is, they resembled the initial 95:5 cell mixture. In contrast, tumours that grew out in wild-type mice consisted of 98% d42m1-T3 tumour cells and lacked mutant spectrin-β2 (Fig. 4g, h). Thus, d42m1 escape tumours develop as a consequence of T-cell-dependent immunoselection favouring the outgrowth of tumour cells that lack major rejection antigens.

This report shows that the combination of cancer exome sequencing and *in silico* epitope prediction algorithms can identify highly immunogenic, tumour-specific mutational antigens in unedited carcinogen-induced cancers that serve as targets for the elimination phase of cancer immunoediting. To our knowledge, this is the first study to use a genomics approach to experimentally identify a tumour antigen, to specifically identify an antigen from an unedited tumour and to demonstrate that T-cell-dependent immunoselection is a mechanism underlying the outgrowth of tumour cells that lack strong rejection antigens. This mechanism most likely also produces other types of escape tumours, such as those that develop inactivating mutations in antigen presentation genes (for example, those encoding MHC class I proteins), which are frequently observed in clinically apparent human cancers[22,23]. Developing carcinogen-induced tumours (for example, mouse MCA sarcomas or human smoker lung cancers) may be the preferred targets of cancer immunoediting because they express the

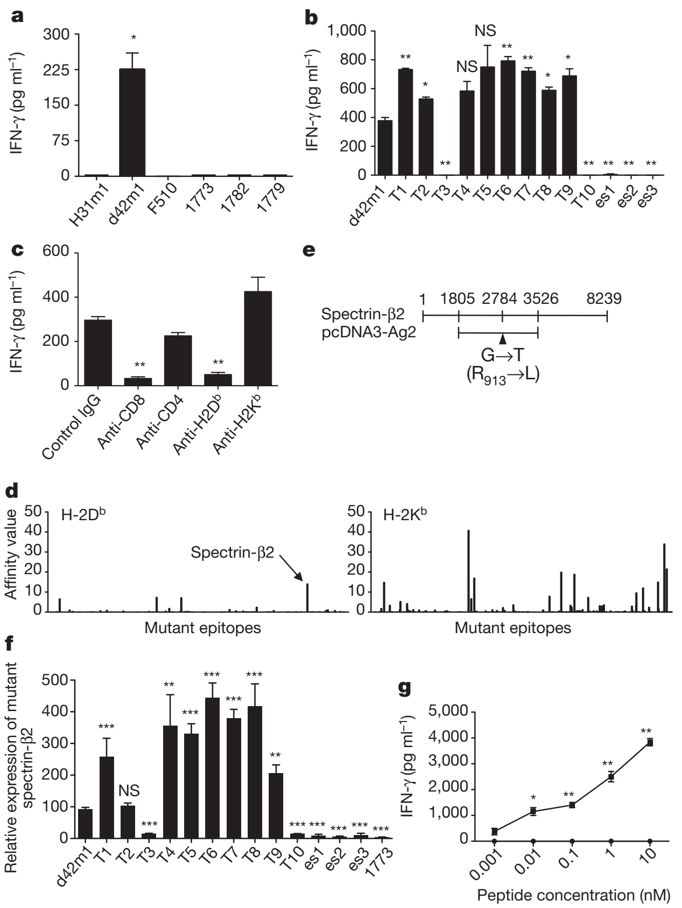

Figure 3 | Identification of mutant spectrin-β2 as an authentic antigen of an unedited tumour. **a**, **b**, IFN-γ release by C3 CTLs following co-culture with different unedited sarcomas (**a**) or d42m1-related tumours (**b**). **c**, IFN-γ release by C3 CTLs is inhibited by monoclonal antibodies that block CD8 and H-2D^b, but not CD4 or H-2K^b. **d**, MHC class I epitopes predicted to be shared in all of the regressor d42m1 tumours, but not in progressor d42m1 tumours. **e**, Representation of the cDNA clone that stimulated C3 CTLs encoding the spectrin-β2 R913L mutation. **f**, qRT–PCR for mutant spectrin-β2 in d42m1-related tumours and 1773. **g**, IFN-γ release by C3 CTLs incubated with COS-D^b cells pulsed with wild-type (circles) or mutant (squares) spectrin-β2 peptides. Data are representative of three independent experiments. Samples were compared in **b**, **f** to d42m1 using an unpaired, two-tailed Student's *t* test (*$P < 0.05$, **$P < 0.01$, ***$P < 0.001$; NS, not significant).

greatest number of mutations that might function as neoantigens. However, as ~1% of the mutations in d42m1 are selectively expressed in regressor tumour clones, it is possible that spontaneous tumours arising by other means that harbour as few as 100–200 mutations could still be susceptible to immunological sculpting as they develop. In this regard it is significant that, as documented in a complementary study reported in this issue[24], oncogene-induced primary sarcomas engineered to express a strong model antigen can also undergo T-cell-dependent immunoediting, resulting in the outgrowth of tumours that escape immune control. It will be interesting in the future to compare the effects of immunity on the antigenic profiles of oncogene- versus carcinogen-induced tumours.

The immunodominance of mutant spectrin-β2 in driving tumour rejection in many ways resembles that of certain viral antigens[25] and is probably due to the presence in d42m1 of four copies of chromosome 11, each of which carries the spectrin-β2 gene, thereby producing a highly abundant neoepitope that binds to H-2D^b 750-fold stronger than that of the wild-type sequence. More work is needed to determine which of the other mutations, if any, selectively expressed in d42m1 regressors function as rejection antigens. Immunoepitope analysis of parental

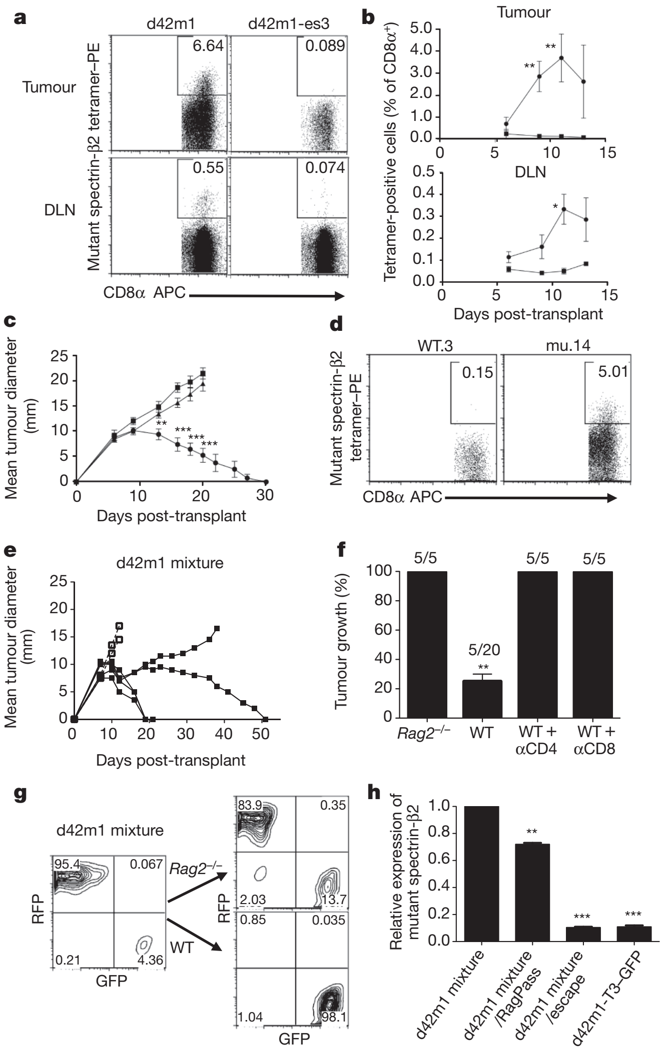

Figure 4 | Mutant spectrin-β2 is a major rejection antigen of d42m1. **a**, Mutant spectrin-β2-specific CD8$^+$ T cells were detected by tetramer staining in tumours and draining lymph nodes (DLNs) from mice challenged with d42m1 parental cells, but not d42m1-es3 cells on day 11 post-transplant. APC, allophycocyanin; PE, phycoerythin. **b**, Quantification and kinetics of mutant spectrin-β2 tetramer staining in mice challenged with d42m1 parental cells ($n = 3$, circles) or d42m1-es3 cells ($n = 3$, squares). **c**, Growth of d42m1-es3 tumour cell clones transduced with wild-type ($n = 5$, squares) or mutant spectrin-β2 ($n = 5$, circles) and control d42m1-es3 cells ($n = 5$, triangles) after transplantation (1×10^6 cells) into wild-type mice. Data are presented as average tumour diameter ± s.e.m. **d**, d42m1-es3 tumours reconstituted with wild-type (WT.3) or mutant spectrin-β2 (mu.14) were harvested at day 11 and CD8α$^+$ T cells were stained with mutant spectrin-β2 tetramers. **e**, Growth of a mixture of d42m1-T2–RFP (95%) and of d42m1-T3–GFP (5%) after transplantation (1×10^6 total cells) into wild-type ($n = 5$, solid lines, closed squares) or *Rag2*$^{-/-}$ ($n = 2$, dashed lines, open squares) mice. **f**, Tumour outgrowth in *Rag2*$^{-/-}$ or wild-type (WT) mice treated or untreated with monoclonal antibodies that deplete CD4$^+$ or CD8$^+$ T cells after challenge with 1×10^6 cells of a d42m1 mixture (95% d42m1-T2–RFP and 5% d42m1-T3–GFP). Data are presented as per cent tumour positive mice from 2–4 independent experiments ($n = 2$–5 mice per group). **g**, **h**, GFP and RFP expression (**g**) and mutant spectrin-β2 expression (**h**) were analysed in the d42m1-T2–RFP/d42m1-T3–GFP tumour cell mixture before injection and from tumours that grew out in *Rag2*$^{-/-}$ mice (RagPass) or escaped in wild-type mice by flow cytometry (**g**) or qRT–PCR (**h**). Data are representative of two independent experiments. Samples were compared using an unpaired, two-tailed Student's *t*-test (*$P < 0.05$, **$P < 0.01$, ***$P < 0.001$; NS, not significant).

H31m1 reveals that it expresses multiple potential strong neoantigens (19 potential strong binders to H-2D^b and 58 to H-2K^b) (Supplementary Fig. 11a) and induces both H-2D^b- and H-2K^b-restricted

$CD8^+$ T-cell responses during rejection (Supplementary Fig. 11b). This result suggests that H31m1 shows an even more complex antigenicity than d42m1 and probably explains why H31m1 never produces escape tumours in wild-type mice (Supplementary Fig. 11c).

Chemically induced tumours have had a critical role in the history of tumour immunology, providing the first unequivocal demonstration of tumour-specific antigens[26,27] and, subsequently, the first evidence of cancer immunoediting[1–3]. It is therefore significant that this same model has now provided new insights into the antigenic targets of cancer immunoediting and some of the key molecular mechanisms that drive the process. Although more work is needed to determine whether and how frequently this process occurs during development of spontaneous and carcinogen-induced human cancers, it is tempting to speculate that a genomics approach to tumour antigen identification could, in the future, facilitate the development of individualized cancer immunotherapies directed at tumour-specific—rather than cancer-associated—antigens.

METHODS SUMMARY

d42m1 and H31m1 MCA-induced sarcomas were generated in male 129/Sv *Rag2*$^{-/-}$ mice as previously described[1]. Total RNA was isolated from low-passage MCA-induced sarcoma cell lines and skin fibroblasts from male 129/Sv *Rag2*$^{-/-}$ mice using the RNeasy Mini kit (Qiagen) and cDNA was prepared using oligo (dT) primers and SuperScript II Reverse Transcriptase (Invitrogen). Illumina libraries prepared with this cDNA were hybridized to biotinylated Agilent mouse exome probes. Library components were captured using strepavidin-coated magnetic beads (DynaBeads), PCR amplified and sequenced using an Illumina GAIIx analyser (cDNA CapSeq). Putative somatic mutations were identified using VarScan 2 (v.2.2.4). Missense mutations were analysed for potential neoepitope binding to MHC class I using an algorithm[20] available at Immune Epitope Database and Analysis Resource (http://www.immuneepitope.org) and were expressed as affinity values (reciprocal of the predicted IC_{50} multiplied by 100).

All tumour cell lines were injected subcutaneously in the flank of naïve syngeneic male mice (1×10^6 cells). Ten d42m1 tumour cell clones were isolated from the parental cell line by limiting dilution. Escape tumours of d42m1 were harvested from tumours growing in wild-type mice and cell lines were produced. To generate the C3 d42m1-specific CTL clone, splenocytes from a mouse that rejected d42m1 were harvested, stimulated with parental d42m1 target cells pre-treated with $100\,U\,ml^{-1}$ IFN-γ for 48 h and irradiated with 100 Gy and cloned by limiting dilution. To clone the antigen recognized by the C3 CTL clone, a d42m1 cDNA library was cloned into pcDNA3 (Invitrogen), transfected into COS cells expressing mouse H-$2D^b$, and screened for C3 reactivity by IFN-γ ELISA (eBioscience). Mutant spectrin-β2 expression was detected by qRT–PCR using mutation-specific primers. H-$2D^b$ tetramers were generated with 905–913 mutant spectrin-β2 peptides by the NIH Tetramer Facility (Emory).

Full Methods and any associated references are available in the online version of the paper at www.nature.com/nature.

Received 17 August; accepted 2 December 2011.
Published online 8 February 2012.

1. Shankaran, V. *et al.* IFNγ and lymphocytes prevent primary tumour development and shape tumour immunogenicity. *Nature* **410,** 1107–1111 (2001).
2. Dunn, G. P., Bruce, A. T., Ikeda, H., Old, L. J. & Schreiber, R. D. Cancer immunoediting: from immunosurveillance to tumor escape. *Nature Immunol.* **3,** 991–998 (2002).
3. Koebel, C. M. *et al.* Adaptive immunity maintains occult cancer in an equilibrium state. *Nature* **450,** 903–907 (2007).
4. Vesely, M. D., Kershaw, M. H., Schreiber, R. D. & Smyth, M. J. Natural innate and adaptive immunity to cancer. *Annu. Rev. Immunol.* **29,** 235–271 (2011).
5. Schreiber, R. D., Old, L. J. & Smyth, M. J. Cancer immunoediting: integrating immunity's roles in cancer suppression and promotion. *Science* **331,** 1565–1570 (2011).
6. Futreal, P. A. *et al.* A census of human cancer genes. *Nature Rev. Cancer* **4,** 177–183 (2004).
7. Chen, A. C. & Herschman, H. R. Tumorigenic methylcholanthrene transformants of C3H/10T1/2 cells have a common nucleotide alteration in the c-Ki-ras gene. *Proc. Natl Acad. Sci. USA* **86,** 1608–1611 (1989).
8. Tuveson, D. A. *et al.* Endogenous oncogenic K-ras(G12D) stimulates proliferation and widespread neoplastic and developmental defects. *Cancer Cell* **5,** 375–387 (2004).
9. Kirsch, D. G. *et al.* A spatially and temporally restricted mouse model of soft tissue sarcoma. *Nature Med.* **13,** 992–997 (2007).
10. Ley, T. J. *et al.* DNA sequencing of a cytogenetically normal acute myeloid leukaemia genome. *Nature* **456,** 66–72 (2008).
11. Ding, L. *et al.* Genome remodelling in a basal-like breast cancer metastasis and xenograft. *Nature* **464,** 999–1005 (2010).
12. Shah, S. P. *et al.* Mutational evolution in a lobular breast tumour profiled at single nucleotide resolution. *Nature* **461,** 809–813 (2009).
13. Lee, W. *et al.* The mutation spectrum revealed by paired genome sequences from a lung cancer patient. *Nature* **465,** 473–477 (2010).
14. Pleasance, E. D. *et al.* A small-cell lung cancer genome with complex signatures of tobacco exposure. *Nature* **463,** 184–190 (2010).
15. Totoki, Y. *et al.* High-resolution characterization of a hepatocellular carcinoma genome. *Nature Genet.* **43,** 464–469 (2011).
16. Puente, X. S. *et al.* Whole-genome sequencing identifies recurrent mutations in chronic lymphocytic leukaemia. *Nature* **475,** 101–105 (2011).
17. Pleasance, E. D. *et al.* A comprehensive catalogue of somatic mutations from a human cancer genome. *Nature* **463,** 191–196 (2010).
18. Boon, T., Coulie, P. G., Van den Eynde, B. J. & van der Bruggen, P. Human T cell responses against melanoma. *Annu. Rev. Immunol.* **24,** 175–208 (2006).
19. Segal, N. H. *et al.* Epitope landscape in breast and colorectal cancer. *Cancer Res.* **68,** 889–892 (2008).
20. Nielsen, M. *et al.* Reliable prediction of T-cell epitopes using neural networks with novel sequence representations. *Protein Sci.* **12,** 1007–1017 (2003).
21. van der Bruggen, P. *et al.* A gene encoding an antigen recognized by cytolytic T lymphocytes on a human melanoma. *Science* **254,** 1643–1647 (1991).
22. Khong, H. T. & Restifo, N. P. Natural selection of tumor variants in the generation of "tumor escape" phenotypes. *Nature Immunol.* **3,** 999–1005 (2002).
23. Dunn, G. P., Old, L. J. & Schreiber, R. D. The three Es of cancer immunoediting. *Annu. Rev. Immunol.* **22,** 329–360 (2004).
24. DuPage, M., Mazumdar, C., Schmidt, L. M., Cheung, A. F. & Jacks, T. Expression of tumour-specific antigens underlies cancer immunoediting. *Nature* doi:10.1038/nature10803 (this issue).
25. Yewdell, J. W. Confronting complexity: real-world immunodominance in antiviral $CD8^+$ T cell responses. *Immunity* **25,** 533–543 (2006).
26. Prehn, R. T. & Main, J. M. Immunity to methylcholanthrene-induced sarcomas. *J. Natl. Cancer Inst.* **18,** 769–778 (1957).
27. Old, L. J. & Boyse, E. A. Immunology of experimental tumors. *Annu. Rev. Med.* **15,** 167–186 (1964).

Supplementary Information is linked to the online version of the paper at www.nature.com/nature.

Acknowledgements We are grateful to J. Archambault for expert technical assistance, T. H. Hansen (Washington University) for providing MHC class I antibodies, S. Horvath and P. M. Allen (Washington University) for synthesizing MHC class I peptides, the National Institutes of Health (NIH) Tetramer Core Facility for producing MHC class I tetramers, and T. S. Stappenbeck (Washington University) for technical help in recovering frozen tumour samples. We also thank E. Unanue, P. M. Allen and J. Bui for criticisms and comments, all members of the Schreiber laboratory for discussions, and the many members of The Genome Institute at Washington University School of Medicine, especially L. Ding for her insights into our analytical approaches. This work was supported by grants to R.D.S. from the National Cancer Institute, the Ludwig Institute for Cancer Research, the Cancer Research Institute, and the WWWW Foundation; and to E.R.M. from the National Human Genome Research Institute. M.D.V. is supported by a pre-doctoral fellowship from the Cancer Research Institute. J.P.A. is supported by the Howard Hughes Medical Institute and the Ludwig Center for Cancer Immunotherapy; M.J.S. by the National Health and Medical Research Council of Australia (NH&MRC) and from the Association for International Cancer Research; and L.J.O. by the Ludwig Institute for Cancer Research and the Cancer Research Institute.

Author Contributions H.M. and M.D.V. were involved in all aspects of this study including planning and performing experiments, analysing and interpreting data, and writing the manuscript. C.G.R., R.U., C.D.A., J.M.W., Y.-S.C. and L.K.S. also performed experiments and analysed data. V.J.M., R.D. and members of The Genome Institute performed Illumina library preparation, cDNA capture and sequencing as well as validation Roche/454 pyrosequencing and 3730 sequencing. D.C.K. analysed and interpreted sequencing data from this study and previously published cancer genome data. J.H. and T.W. analysed cDNA CapSeq data for potential MHC class I epitopes. M.C.W. performed the phylogenetic analysis on the tumour cells. J.P.A., M.J.S. and L.J.O. interpreted data and contributed to the preparation of the final manuscript. E.R.M. and R.D.S oversaw all the work performed, planned experiments, interpreted data and wrote the manuscript.

Author Information Reprints and permissions information is available at www.nature.com/reprints. The authors declare no competing financial interests. Readers are welcome to comment on the online version of this article at www.nature.com/nature. Correspondence and requests for materials should be addressed to R.D.S. (schreiber@immunology.wustl.edu).

METHODS

Mice. *Ifngr1*$^{-/-}$ mice[28] and *Ifnar1*$^{-/-}$ mice[29] on a 129/Sv background were originally provided by M. Aguet and were bred in our specific pathogen-free animal facility. Wild-type and *Rag2*$^{-/-}$ mice were purchased from Taconic Farms. All mice were male and on a 129/Sv background and were housed in our specific pathogen-free animal facility. For all experiments, male mice were 8–12 weeks of age and studies were performed in accordance with procedures approved by the AAALAC accredited Animal Studies Committee of Washington University in St. Louis.

Tumour transplantation. MCA-induced sarcomas used in this study were generated in male 129/Sv strain wild-type or *Rag2*$^{-/-}$ mice and banked as low-passage tumour cells as previously described[1]. Tumour cells derived from frozen stocks were propagated *in vitro* in RPMI media (Hyclone) supplemented with 10% FCS (Hyclone) and injected subcutaneously in 150 μl of endotoxin-free PBS into the flanks of recipient mice. Tumour cells were >90% viable at the time of injection as assessed by trypan blue exclusion and tumour size was quantified as the average of two perpendicular diameters. For antibody depletion studies, 250 μg of control IgG (PIP), anti-CD4 (GK1.5) or anti-CD8α (YTS169.4) were injected intraperitoneally into mice at day −1 and every 7 days thereafter.

Isolation of normal skin fibroblasts. Skin fibroblasts were isolated from three independent male 129/Sv *Rag2*$^{-/-}$ pups by harvesting skin and incubating in 0.25% trypsin (Hyclone) at 37 °C for 30 min before washing in DMEM media (Hyclone). After washing, chunks of skin were filtered to achieve single-cell suspensions and cultured *in vitro* with DMEM media. After three passages, skin fibroblasts were harvested to isolate genomic DNA and total RNA.

Extraction of genomic or complementary DNA. Genomic DNA from sarcoma cells and normal skin fibroblasts was extracted using DNeasy Blood & Tissue Kit (Qiagen). For cDNA isolation, total RNA from sarcoma cells and normal skin fibroblasts was isolated using RNeasy Mini kit (Qiagen) and cDNA was synthesized using oligo (dT) primers and SuperScript II Reverse Transcriptase (Invitrogen).

cDNA CapSeq. cDNA samples from each tumour (100 ng) were constructed into Illumina libraries according to the manufacturer's protocol (Illumina) with the following modifications. First, cDNA was fragmented using Covaris S2 DNA Sonicator (Covaris) in 1× end-repair buffer followed by the direct addition of the enzyme repair cocktail (Lucigen). Fragment sizes ranged between 100–500 bp. Second, Illumina adaptor-ligated DNA was amplified in four 50 μl PCRs for five cycles using 4 μl adaptor-ligated cDNA, 2× Phusion Master Mix and 250 nM forward and reverse primers, 5′-AATGATACGGCGACCACCGAGATCTACACTCTTTCCCTACACGACGCTCTTCCGATC and 5′- CAAGCAGAAGACGGCATACGAGATGTGACTGGAGTTCAGACGTGTGCTCTTCCGATC, respectively. Third, Solid Phase Reversible Immobilization (SPRI) bead cleanup was used to purify the PCR-amplified library and to select for 300–500 bp fragments. Five-hundred nanograms of the size-fractionated Illumina library were hybridized with the Agilent mouse exome reagent. After hybridization at 65 °C for 24 h, we added 50 μl of DynaBeads M-270 streptavidin-coated paramagnetic beads (10 mg ml^{-1}) to selectively remove the biotinylated Agilent probes and hybridized cDNA library fragments. The beads were washed according to manufacturer's protocol (Agilent) and the captured library fragments were released into solution using 50 μl of 0.125 N NaOH and neutralized with an equal volume of neutralization buffer (Agilent). The recovered fragments then were PCR amplified according to the manufacturer's protocol using 11 cycles in the PCR. Illumina library quantification was completed using the KAPA SYBR FAST qPCR Kit (KAPA Biosystems). The qPCR result was used to determine the quantity of library necessary to produce 180,000 clusters on a single lane of the Illumina GAIIx. One lane of 100 bp paired-end data was generated for each captured sample (as cDNA was used as the source for sequencing, we refer to this process as cDNA Capture Sequencing or cDNA CapSeq). Illumina reads were aligned to the NCBI build 37 (Mm9) mouse reference sequence using BWA[30] v.0.5.5 (with –q 5 soft trimming). Alignments from multiple lanes for the same sample were merged together using SAMtools r599, and duplicates were marked using Picard v.1.29.

Mutation detection and annotation. Putative somatic mutations were identified using VarScan 2 (v.2.2.4)[31] with the parameters '–min-coverage 3–min-var-freq 0.08–p-value 0.10–somatic-p-value 0.05–strand-filter 1' and specifying a minimum mapping quality of 10. Variants whose supporting reads exhibited read position bias (average read position <10 or >90), strand bias (>99% of reads on one strand), or mapping quality (score difference >30, or mismatch quality sum difference >100) relative to reference supporting reads were removed as probable false positives. We also required that the variant allele be present in at least 10% of tumour reads and no more than 5% of normal reads. The SNVs meeting these criteria were annotated using an internal database of GenBank/Ensembl transcripts (v58_73k). In the event that a variant was annotated using multiple transcripts, the annotation of most severe effect was used. Non-silent coding mutations (missense, nonsense/nonstop or splice site) were prioritized for downstream analysis.

Mutation rate and overlap comparisons. Mutation rates were estimated for each tumour sample using the number of putative 'tier 1' SNVs (missense, nonsense/nonstop, splice site, silent or noncoding RNA). To account for variability in coverage between samples, the SNV count for each tumour sample (S) was divided by a coverage factor (F), computed as the fraction of all tier 1 SNVs identified in any tumour sample ($n = 16{,}991$) that were covered by at least four reads in a given sample. For example, in the d42m1 parental sample, 15,852 of 16,991 tier 1 SNV positions were covered, for a coverage factor of 93.30%. The number of coverage-adjusted mutations in each sample was divided by the total size of tier 1 space in the mouse genome (43.884 Mbp) to determine the number of coding mutations per megabase (R).

$$R = (S/F) / (43.884\ \mathrm{Mbp})$$

For the mutation overlap comparisons and relatedness-to-parental-tumour analysis, only high-confidence missense mutations were used (that is, 20× or above). A mutation was considered 'shared' between two samples if both samples had a predicted mutation at the same genomic position. For the comparison of mutated genes between d42m1 and H31m1 parental lines, a gene was considered 'shared' if both d42m1 and H31m1 samples had a predicted missense mutation in that gene, even if the mutations did not occur at the same position.

Roche/454 sequencing and validation. PCR primers were designed for 11 SNVs predicted to be somatic in d42m1 tumour samples, as well as 11 control sites that were H31m1-specific, low-confidence, or removed by the false-positive filter. All 22 SNVs were PCR amplified individually in 11 samples (SK1.1, d42m1, H31m1, T2, T3, T5, T9, T10, es1, es2 and es3) using MID-tailed primers to enable sample identification. PCR products were pooled together before sequencing on a quarter run of the Roche/454 Titanium platform. Read sequences and quality scores were extracted from 454 data files using *sffinfo* (454 proprietary software) then aligned to the mouse build 37 reference sequence (Mm19) using SSAHA2 v.2.5.3[32] with the SAM output option. Alignments were imported to BAM format and a 'pileup' assembly file generated using SAMtools v.0.1.18[33]. The average 454 sequence depth for targeted positions was 1,216× per sample. Validation read counts and allele frequencies in each sample at each variant position were determined using the *pileup2cns* command of VarScan v.2.2.7[31]. At least 20 reads with base quality of 20 or higher were required to confirm or refute a variant. 454 sequencing data and the primers used are presented in Supplementary Table 4.

3730 sequencing and validation. Eight SNVs predicted to be somatic were selected for validation by PCR and 3730 sequencing in flow-sorted CD45^{+} and CD45^{-} cells from the original d42m1 tumour. Genomic DNA and cDNA from CD45^{-} (tumour) cells, and cDNA from CD45^{+} (normal immune) cells were used for PCR amplification and then PCR products were sequenced individually on ABI 3730 using universal primers. Manual review was performed using amplicon-based assembly in the Integrative Genomics Viewer (IGV)[34] to determine the somatic status for each site. Data are presented in Supplementary Table 4.

MHC class I epitope prediction. All missense mutations for each d42m1-related tumour or H31m1 were analysed for the potential to form MHC class I neoepitopes that bind to either H-2D^{b} or H-2K^{b} molecules. The artificial neural network (ANN) algorithm provided by the Immune Epitope Database and Analysis Resource (http://www.immuneepitope.org) was used to predict epitope binding affinities[20] and the results were ultimately expressed as affinity values ($1/IC_{50} \times 100$). Predicted strong affinity epitopes expressed in d42m1 regressor tumours are listed in Supplementary Table 5.

Phylogenetic analysis of tumour samples. Sequencing data from normal *Rag2*$^{-/-}$ fibroblasts, d42m1 parental cells, d42m1 regressor clones, d42m1 progressor clones, d42m1 escape tumours and H31m1 tumour cells were compared using PHYLogeny Inference Package (PHYLIP)[35] to generate a phylogenetic tree displaying the relatedness of each sample.

Antibodies. Anti-H-2K^{b} (B8-24-3) and anti-H-2D^{b} (B22/249) monoclonal antibodies were provided by T. H. Hansen (Washington University School of Medicine). Anti-CD4 (GK1.5), anti-CD8α (YTS169.4) monoclonal antibodies and control immunoglobulin (PIP, a monoclonal antibody specific for bacterial glutathione *S*-transferase) were produced from hybridoma supernatants and purified in endotoxin-free form by Protein G affinity chromatography (Leinco Technologies). Purified Rat IgG was purchased from Sigma (St. Louis). CD45–FITC, CD45–PE, CD8–APC and purified anti-CD16/32 were purchased from BioLegend.

cDNA library construction and screening. To generate a d42m1 tumour cell cDNA library, mRNA was isolated from parental d42m1 tumour cells using a QuickPrep mRNA Purification kit (Amersham), converted into cDNA using SuperScript II First Strand Synthesis System (Invitrogen) and inserted into the EcoRI site of the expression vector pcDNA3 (Invitrogen). The cDNA library was divided into pools of 100 bacterial colonies with 200–300 ng of DNA from each pool transfected into 2.5×10^4 monkey COS cells engineered to ectopically express mouse H-2D^b (COS-D^b) cells using Lipofectamine 2000. After 48 h, 5×10^3 C3 CTL cells were added, and supernatants were assayed for IFN-γ release 24 h later by ELISA. A single positive cDNA clone was isolated after screening 120,000 cDNA colonies. The putative H-2D^b-binding peptide VAVVNQIAL was predicted using the algorithm available at the Immune Epitope Database and Analysis Resource, http://www.immuneeptiope.org/. The peptides were produced by P. Allen and S. Horvath (Washington University School of Medicine).

Expression vectors. Full-length cDNA encoding wild-type spectrin-β2 and mutant spectrin-β2 were cloned from parental d42m1 tumour cells by RT–PCR using primer pairs 5′-TGAGACAGTCAAGATGACGACCACGGTAGCCACA-3′ and 5′-CGGGACAACAGGGAAGTTCACTTCTTCTTGCCGA-3′. Wild-type and mutant spectrin-β2 cDNA were subcloned from the TOPO-XL vector (Invitrogen) into the retrovirus (RV)–GFP vector[36]. To generate the RV–RFP vector, full-length cDNA encoding RFP was cloned from the pTurboRFP-C vector (Evrogen) by RT–PCR using primer pairs 5′- ATCTCAGAATTCATGAGC GAGCTGATCAAGGA-3′ and 5′-ATCTCAGGATCCTTATCTGTGCCCCA GTTTGCTAG-3′. RFP cDNA was then cloned into the RV vector. To remove candidate T-cell epitopes in RFP, the nucleotide A was replaced by G at position 334 in the cDNA, resulting in amino acid substitution N112D. Coding sequences of the constructs were verified by DNA sequencing (Big Dye method; Applied Biosciences). The dominant-negative version of the IFNGR1 subunit (IFNGR1ΔIC) was expressed into H31m1 and d42m1 tumour cells as previously described[37].

Establishment of CTL lines and clones. To generate the d42m1-specific C3 CTL clone, wild-type mice were injected with 1×10^6 parental d42m1 tumour cells. Fourteen days later, the spleen was harvested from a mouse that rejected the tumour and a CTL line was established by stimulating 40×10^6 splenocytes with 2×10^6 parental d42m1 tumour cells pre-treated for 48 h with 100 U ml^{-1} of recombinant murine IFN-γ and irradiated (100 Gy). After CD8$^+$ T-cell purification using magnetic beads (Miltenyi Biotec) and limiting dilution, the CTL clone C3 was obtained.

Measurement of IFN-γ production. To generate target cells, tumour cells were treated with 100 U ml^{-1} IFN-γ for 48 h and irradiated with 100 Gy before use. The C3 CTL clone was co-cultured at the indicated ratios with target tumour cells (10,000 or 5,000 cells) in 96-well round-bottomed plates overnight. IFN-γ in supernatants was quantified using an IFN-γ ELISA kit (eBioscience). For blocking assays, 10 μg ml^{-1} of anti-CD8 (YTS-169.4), anti-CD4 (GK1.5) or control immunoglobulin (PIP) were added to the cell culture of effector (C3 CTL clone) and target cells (tumours).

Cytotoxicity assay. To generate target cells, tumour cells were treated with 100 U ml^{-1} rMuIFN-γ for 48 h before use. One million tumour cells were labelled with 25 μCi of $Na_2{}^{51}CrO4$ (PerkinElmer) for 90 min at 37 °C, washed and 10,000 cells seeded per well in 96-well round-bottom plates. The C3 CTL clone was co-cultured with the tumour target cells at the indicated effector/target cell ratios and incubated for 4 h at 37 °C in 5% CO_2. Radioactivity was detected in the supernatants and per cent specific killing was defined as (experimental condition c.p.m. − spontaneous c.p.m.) / (maximal (detergent) c.p.m. − spontaneous c.p.m.) × 100. Data points were obtained in duplicate.

Fluorescence-activated cell sorting analysis. For flow cytometry, cells were stained for 20 min at 4 °C with 500 ng of Fc block (anti-CD16/32) and 200 ng of CD45, CD4 or CD8α in 100 μl of staining buffer (PBS with 1% FCS and 0.05% NaN_3 (Sigma)). Propidium iodide (PI) (Sigma) was added at 1 μg ml^{-1} immediately before FACS analysis. For quantitative analysis of tumour-infiltrating lymphocytes/leukocytes (TIL) and lymph node populations, a CD45$^+$ PI$^-$ gate was used and gated events were collected on a FACSCalibur (BD Biosciences) and analysed using FloJo software.

Tumour, draining lymph node and spleen harvest. After tumour cell transplantation, established tumours were excised from mice, minced and treated with 1 mg ml^{-1} type IA collagenase (Sigma) in HBSS (Hyclone) for 2 h at room temperature (22 °C). The ipsilateral inguinal tumour draining lymph nodes and spleen were also harvested and crushed between two glass slides and vigorously resuspended to make single-cell suspensions.

Tetramers. H-2D^b tetramers conjugated to PE were prepared with mutant spectrin-β2 peptides and produced by the NIH Tetramer Core Facility (Emory University).

Mutation-specific RT–PCR and real-time RT–PCR. Total RNA from tumour cells was isolated by RNeasy Mini kit (Qiagen) and cDNA was synthesized from the total RNA using oligo (dT) primers and SuperScript II Reverse Transcriptase (Invitrogen). Real-time PCR specific for wild-type spectrin-β2, mutant spectrin-β2 and GAPDH using the SYBR Green Mastermix kit (Applied Biosystems) were performed on ABI 7000. The primer sequences for used for mutant spectrin-β2 are 5′-GGTGAACCAGATTGCACT-3′ and 5′-TGTCCACCAGTTCTCTGAACT-3′.

Detection of mutation in spectrin-β2 cDNA. The point mutation in the spectrin-β2 gene creates a PstI restriction site (CGGCAG to CTGCAG, underlined letters indicate the site of mutation). To amplify spectrin-β2 cDNA we used a forward primer (ACCCTGGCCCTGTACAAGAT) and reverse primer (TAGACTCGATGACCTTGGTCT). The PCR conditions used were 94 °C for 2 min, followed by 35 cycles of 94 °C for 30 s, 55 °C for 30 s and 72 °C for 30 s. The PCR products were digested for 2 h at 37 °C with PstI restriction enzyme, which cleaved mutant spectrin-β2, but not wild-type spectrin-β2, and generates a 200 bp fragment from cDNA. The products were resolved by electrophoresis on a 1.2% agarose gel and visualized by ethidium bromide staining.

Isolation of non-transformed cells from d42m1 biopsy. A frozen d42m1 tumour biopsy from the original d42m1 tumour was thawed and treated with 1 mg ml^{-1} type IA collagenase (Sigma) in HBSS for 2 h at room temperature. After filtration, single-cell suspensions were stained for 20 min at 4 °C with 500 ng of Fc block (anti-CD16/32) and 200 ng of CD45-PE in 100 μl of staining buffer. Propidium iodide was added at 1 μg ml^{-1} immediately before sorting. A CD45$^+$ PI$^-$ gate was used and the top 15% and the bottom 15% of gated events were collected using a FACSAria II (BD Biosciences). Sorted CD45$^+$ cells (host leukocytes) and CD45$^-$ cells (primary d42m1 tumour cells) were collected and genomic DNA as well as RNA was isolated to synthesize cDNA for 3730 sequencing to validate that the mutation calls detected by Illumina were somatic and tumour specific.

Statistical analysis. Samples were compared using an unpaired, two-tailed Student's *t*-test, unless specified.

28. Huang, S. *et al.* Immune response in mice that lack the interferon-γ receptor. *Science* **259,** 1742–1745 (1993).
29. Muller, U. *et al.* Functional role of type I and type II interferons in antiviral defense. *Science* **264,** 1918–1921 (1994).
30. Li, H. & Durbin, R. Fast and accurate short read alignment with Burrows–Wheeler transform. *Bioinformatics* **25,** 1754–1760 (2009).
31. Koboldt, D. C. *et al.* VarScan: variant detection in massively parallel sequencing of individual and pooled samples. *Bioinformatics* **25,** 2283–2285 (2009).
32. Ning, Z., Cox, A. J. & Mullikin, J. C. SSAHA: a fast search method for large DNA databases. *Genome Res.* **11,** 1725–1729 (2001).
33. Li, H. *et al.* The Sequence Alignment/Map format and SAMtools. *Bioinformatics* **25,** 2078–2079 (2009).
34. Robinson, J. T. *et al.* Integrative genomics viewer. *Nature Biotechnol.* **29,** 24–26 (2011).
35. Felsenstein, J. Phylogeny Inference Package. *Cladistics* **5,** 164–166 (1989).
36. Ranganath, S. *et al.* GATA-3-dependent enhancer activity in *IL-4* gene regulation. *J. Immunol.* **161,** 3822–3826 (1998).
37. Dighe, A. S., Richards, E., Old, L. J. & Schreiber, R. D. Enhanced *in vivo* growth and resistance to rejection of tumor cells expressing dominant negative IFNγ receptors. *Immunity* **1,** 447–456 (1994).